Renewable Energy, Environment, and Power Quality Journal (REE&PQJ)
ISSN:3020-531X
Volume 26, July 2026

Enhancing the Power Control of Wind Turbines in the Pitch Region Using PSO-Optimized Fuzzy Controller

Mohammad Sadeghi[1], J. Enrique Sierra-García[1], Matilde Santos[2] and Lei Ren[3]

[1] Department of Digitalization, University of Burgos, Burgos, Spain, msadeghi.mut@gmail.com, jesierra@ubu.es

[2] Institute of Knowledge Technology, Complutense University of Madrid, Madrid, Spain, msantos@ucm.es

[3] College of Mechanics and Engineering Science, Hohai University, Nanjing, 211100(China), RyanL177@outlook.com

Abstract. Wind turbines operate under highly nonlinear and uncertain conditions caused by complex aerodynamics and wind-speed variability, making stable power regulation challenging. This paper proposes a unified pitch control strategy based on a Fuzzy Logic Controller (FLC), whose membership functions and control parameters are optimally tuned using the Particle Swarm Optimization (PSO) algorithm to improve power regulation stability under wind variations. A detailed nonlinear dynamic wind turbine model is developed in MATLAB/Simulink, incorporating spatial and lag filters for enhanced aerodynamic accuracy. Classical PID and fuzzy pitch controllers are designed and compared. The PSO-based tuning is performed using a cost function that accounts for power-tracking accuracy and system stability. Simulation results under constant and time-varying wind conditions show that the proposed PSO-optimized FLC achieves lower tracking error, smoother dynamic response, and improved stability compared with the conventional PID controller. These results demonstrate the effectiveness of the proposed approach for robust wind turbine power control.

Key words. Modeling, Intelligent control, Fuzzy Logic Controller, Particle Swarm Optimization, Wind Turbine.

1. Introduction

With the increasing penetration of wind energy into modern power grids, the design of stable and efficient control systems for wind turbines under real operating conditions has become a critical challenge. This challenge arises from the inherently nonlinear and uncertain dynamics of wind turbines, which are continuously affected by stochastic wind variations and, in offshore environments, by wave-induced disturbances [1]. Controllers based on linearized models or conventional PID strategies often exhibit limited adaptability to these conditions, leading to power fluctuations, increased structural fatigue, and reduced energy conversion efficiency [2].

To overcome these limitations, fuzzy logic (FL)–based control has emerged as a flexible and knowledge-driven approach capable of handling nonlinearities and uncertainties. In particular, FL combined with conventional PI controllers in individual pitch control (IPC) schemes has demonstrated effective reduction of unbalanced structural loads while maintaining power stability [3]. This concept has been further extended to hybrid architectures, such as Fuzzy–LQR/PI controllers, which have achieved significant suppression of platform motion and blade bending moments in floating offshore wind turbines (FOWTs) [4]. Beyond structural load mitigation, fuzzy logic has also been successfully applied to grid-support functions. Its integration into droop and inertia control loops, together with pitch angle control, has improved the frequency response of variable-speed wind turbines (VSWTs) [5]. Moreover, fuzzy PID–based IPC strategies relying on effective wind speed estimation have been shown to reduce blade loads while maintaining rated power under turbulent offshore wind conditions [6].

In parallel, reinforcement learning (RL) has gained attention as a data-driven framework for autonomous controller tuning in complex and uncertain environments. RL-based optimization of fuzzy controller membership functions has demonstrated superior power regulation performance compared to fixed fuzzy controllers and classical PID schemes [7]. However, challenges such as slow convergence and oscillatory learning behavior have motivated the development of hybrid RL-based architectures. For example, combining an RL controller with a baseline PID and an intelligent learning observer has improved convergence speed and overall efficiency [8].

Metaheuristic optimization techniques constitute a third paradigm for controller tuning, offering systematic and computationally efficient solutions to multi-objective control problems. Among these methods, Particle Swarm Optimization (PSO) has been widely adopted for wind turbine control applications. PSO-based optimization has been successfully applied to minimize platform motion while maximizing power output in FOWTs, achieving substantial reductions in platform pitch oscillations [9]. The effectiveness of PSO in tuning fuzzy controller parameters has also been validated in other highdimensional nonlinear systems, such as satellite attitude control, where PSO-optimized fuzzy–quaternion controllers demonstrated robust performance under significant parameter uncertainties [10]. These results strongly motivate the application of PSO-based fuzzy control to wind turbine pitch regulation.

In addition to intelligent and optimization-based methods, robust control approaches have been proposed to explicitly address combined wind–wave disturbances and model uncertainties. Event-triggered H∞ pitch control strategies have been shown to maintain system stability while reducing computational burden under high disturbance levels [11]. Similarly, model-dependent extended state observer–based active disturbance rejection controllers (ADRCs) have been developed to estimate and compensate for total disturbances in real time, enhancing operational robustness [12].

Despite these advances, existing approaches typically focus on a limited subset of the interconnected control objectives, such as power regulation, load mitigation, or platform motion suppression [13]. A clear research gap remains in the development of a unified control framework capable of simultaneously addressing these competing objectives under realistic operating conditions and combined disturbances. This challenge is further compounded by practical constraints such as pitch actuator saturation, which can degrade controller performance even within nominal operating ranges [14].

To address this gap, this paper proposes a unified pitch control strategy based on a fuzzy logic controller (FLC) whose membership functions and control parameters are optimally tuned using the Particle Swarm Optimization (PSO) algorithm. The proposed PSO-optimized FLC is designed to enhance power regulation stability under wind-speed variations and system nonlinearities. Its performance is evaluated and compared with that of a conventional PID controller through comprehensive numerical simulations.

The remainder of this paper is organized as follows. Section 2 presents the dynamic modeling of the wind turbine system. Section 3 describes the design of the baseline PID and fuzzy logic controllers. Section 4 introduces the PSO optimization method. Section 5 details the proposed PSO-optimized fuzzy controller. Section 6 presents the simulation setup, results, and comparative analysis. Finally, Section 7 concludes the paper and outlines directions for future research.

2. Wind Turbines Dynamic Modeling

In this study, a 7-kW wind turbine is considered as the reference system. The mathematical model of this small-scale wind turbine is described by Equations (1)–(9) [8]. The electrical output power of the generator is calculated as:

$$P_{out} = R_L . I_a{}^2 \tag{1}$$

Where R_L is the load resistance, and I_a is the armature current. The dynamic equation of the armature current is expressed as:

$$\dot{I}_a = \frac{1}{L_a}\left(K_g \,.\, K_\phi \,.\, \omega \; - (R_a + R_L).I_a\right) \tag{2}$$

Where L_a and R_a denote the armature inductance and armature resistance, respectively. Also, K_g is the dimensionless generator constant, K_ϕ is the magnetic flow coupling constant, and ω is the rotor angular speed. The dynamic equation of the rotor angular speed is given by:

$$\dot{\omega} = \frac{1}{2\,.J\,.\omega}\left(C_p(\lambda_i\,,\theta).\rho\,\pi\,R^2.v_{ef}^3\right) - \frac{1}{J}\left(K_g.K_\phi.I_a + K_f.\omega\right) \tag{3}$$

Where J is the rotational inertia, ρ is the air density, R is the blade radius, v_{ef} is the effective wind speed acting on the blades, and K_f is the friction coefficient. Moreover, C_p is the dimensionless power coefficient of the wind turbine, which is obtained as:

$$C_p(\lambda_i\,,\theta) = c_1\left[\frac{c_2}{\lambda_i} - c_3\theta - c_4\theta^{c_5} - c_6\right]e^{-\frac{c_7}{\lambda_i}} \tag{4}$$

Where $c_1, c_2, c_3, c_4, c_5, c_6, c_7$ are constant coefficients and the parameter λ_i is calculated as:

$$\lambda_i = [\left(\frac{1}{\lambda + c_8}\right) - \left(\frac{c_9}{\theta^3 + 1}\right)]^{-1} \tag{5}$$

Where c_8 and c_9 are constant coefficients. The blade pitch angle computed as:

$$\ddot{\theta} = \frac{1}{T_\theta}[K_\theta(\theta_{ref} - \theta) - \dot{\theta}] \tag{6}$$

Where K_θ and T_θ are the dimensionless parameters of the pitch actuator. Also, the tip-speed ratio (TSR) or λ is obtained as:

$$\lambda = (\omega\,.R)/v_{ef} \tag{7}$$

Where the v_{ef} or effective wind speed acting on the blades is calculated as:

$$v_{ef} = f_{blade}(v_w) \tag{8}$$

Where:

$$f_{blade}(s) = \frac{\beta.s + \sqrt{2}}{\beta^2.s^2\left(\sqrt{\left(\frac{2}{\alpha}\right)} + \sqrt{\alpha}\right).\beta.s + \sqrt{2}} \cdot \frac{\gamma.s + 1/\tau}{s + 1/\tau} \tag{9}$$

In these equations, α, β, γ, and τ are the parameters of the spatial and Lag filters. The numerical values of the wind turbine parameters used in the simulations are listed in Table I, which are extracted from [8]. This small-scale wind turbine has been widely used in previous studies, allowing a fair and consistent comparison of simulation results.

Table I. Parameters of the wind turbine model

Parameters	Value/Units
L_a	13.5 *mH*
K_g	23.31
K_ϕ	0.264 *V/rad/s*
R_a	0.275 Ω
R_L	8 Ω
J	6.53 Kgm^2
R	3.2 *m*
P	1.223 Kg/m^3
K_f	0.025 *N m/rad/s*
[c_1, c_2, c_3]	[0.73, 151, 0.58]
[c_4, c_5, c_6]	[0.002, 2.14, 13.2]
[c_7, c_8, c_9]	[18.4, -0.02, -0.003]
[K_θ, T_θ]	[0.15, 2]
[α, β, γ, τ]	[0.55, 0.832, 1.17, 9]

3. Control Structure

After implementing the complete nonlinear dynamic equations of the wind turbine in MATLAB/Simulink, an appropriate control strategy must be designed to regulate the output power. In this paper, a dual-loop control structure is adopted to enhance the stability and performance of the control system. In this configuration (Fig. 1), an inner-loop controller is first designed for the pitch actuator. In contrast, an outer-loop controller regulates the wind turbine's generated power.

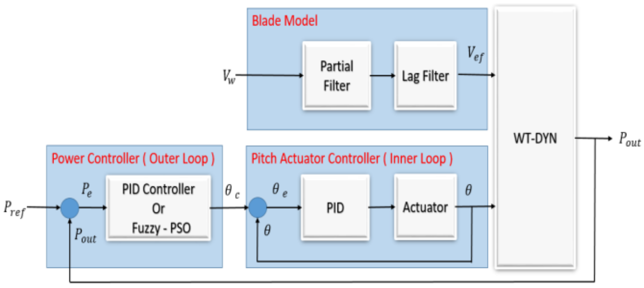

Fig. 1. Main Control strategy

In the inner loop, a classical controller is applied (Fig. 2), which provides satisfactory stability and dynamic performance. In this controller, the gains $K_p = 2.230$, $K_I = 0.426$, and $K_d = 2.817$ have been used.

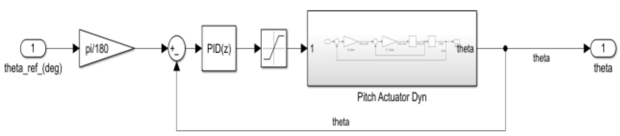

Fig. 2.Pitch Actuator Controller (Inner loop)

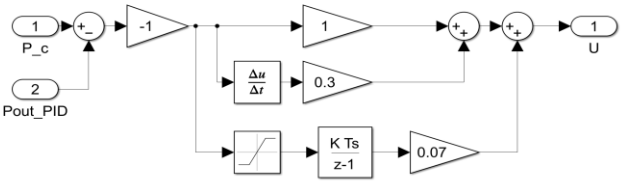

Fig. 3. PID Power Controller (Outer loop)

In the outer loop or power controller, two control strategies, including a conventional PID controller (Fig. 3) with gains $K_p = 1$, $K_I = 0.07$ and $K_d = 0.3$, and a fuzzy controller optimized using the PSO algorithm (Fig. 4), are investigated [10].

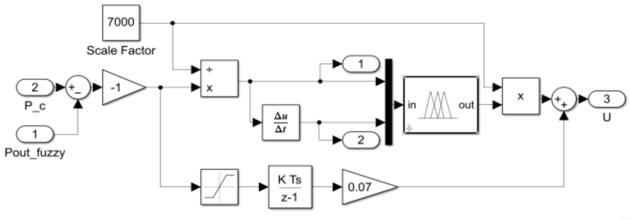

Fig. 4.Fuzzy Power Controller (Outer loop)

The main objective of this study is to compare the performance of these two controllers in terms of power regulation accuracy, oscillation reduction, and improved transient response.

4. Particle Swarm Optimization Algorithm

Particle Swarm Optimization is a stochastic metaheuristic optimization algorithm inspired by the collective behavior of a swarm. In this algorithm, each particle has a position and a velocity, which are iteratively updated using both the particle's personal best and the swarm's global best position. The new position of each particle is obtained by adding its velocity vector to its current position. This process is repeated until convergence to the global optimal solution is achieved.

The velocity and position update equations are given as:

$$v_i(K+1) = w.\, v_i(K) + C_1.r_1(k)(x_g - x_i(K)) + C_2.r_2(k)(\,x_i^P - x_i(K)) \quad (10)$$

$$x_i(K+1) = x_i(K) + v_i(K+1) \quad (11)$$

Where $v_i(K)$ is the velocity of particle i at iteration K, w is the inertia weight, x_i is the personal best position, $x_g$is the global best position, and C_1, C_2 are acceleration coefficients. The random numbers r_1 and r_2 are uniformly distributed in the interval [0-1]. To reduce the search time, the search space is bounded within predefined limits.

The cost function used for the optimization process is defined as:

$$F = \int (x^T Q x + u^T R u) dt \quad (12)$$

Where x represents the tracking error, u is the control signal, and Q and R are weighting matrices selected by the designer.

5. PSO-Optimized Fuzzy Controller

The proposed fuzzy controller is designed based on the power tracking error and its derivative, replacing a classical PD controller. Accordingly, the fuzzy rules are defined using these two inputs and based on the experience obtained from the dynamic responses of the system. To achieve optimal performance, the Mamdani inference method with the Minimum (AND) operator is adopted [10].

In the first step of the fuzzy controller design, the shape and number of membership functions (MFs) are determined. Previous studies have shown that complex membership functions are not suitable for fuzzy tuning algorithms and increase the computational burden in real-time applications. Therefore, triangular membership functions are selected in this work. Seven preset membership functions, including Large Negative (LN), Medium Negative (MN), Small Negative (SN), Zero (ZE), Small Positive (SP), Medium Positive (MP), and Large Positive (LP), are considered for both two inputs and output, corresponding to the linguistic variables (Fig. 5).

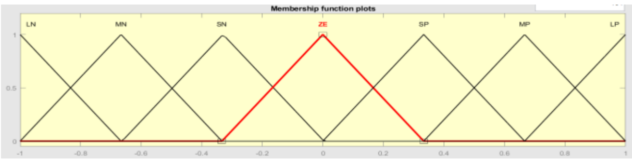

Fig. 5. Consideration of membership functions for each input and output

In the second step, the fuzzy rules are derived. As mentioned earlier, the proposed fuzzy rules are developed based on the designer's experience and inspired by the PD controller structure. The fuzzy controller utilizes two inputs, including the power error (e) and its rate ($\dot{e}$). Since seven membership functions are selected for each input, a total of 49 fuzzy rules are defined in Table II.

Table II. Fuzzy rules definition

		E_dot						
		LN	**MN**	**SN**	**ZE**	**SP**	**MP**	**LP**
E	**LN**	LN	LN	MN	MN	SN	SN	ZE
	MN	LN	MN	MN	SN	SN	ZE	SP
	SN	MN	MN	SN	SN	ZE	SP	SP
	ZE	MN	SN	SN	ZE	SP	SP	MP
	SP	SN	SN	ZE	SP	SP	MP	MP
	MP	SN	ZE	SP	SP	MP	MP	LP
	LP	ZE	SP	SP	MP	MP	LP	LP

The fuzzy control output surface (Fig. 6) is generated by the fuzzy rules and membership functions.

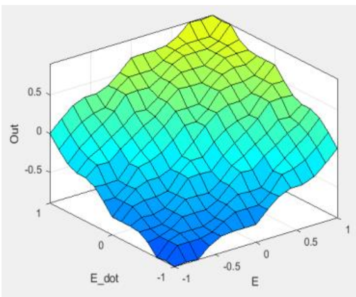

Fig. 6. Fuzzy control output surface

In the third step, the tuning of the fuzzy membership functions by changing the triangular point is performed. Since trial-and-error tuning is a time-consuming and inefficient process, the PSO algorithm is employed to optimally adjust the membership functions based on a predefined cost function.

In order to eliminate the steady-state error in the shortest possible time, the time variable is also incorporated into the objective function. Accordingly, the objective function is defined as Equation 13.

$$O.F = \int\left(t.\sqrt{e^2 + \dot{e}^2} \right)dt \tag{13}$$

The objective function is implemented in the Simulink environment (Fig. 7).

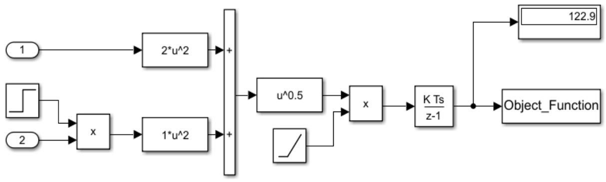

Fig. 7. Implemented objective function

The main task of the optimization process in this method is to determine the defining points of the triangular membership functions for both the inputs and the output. Therefore, the membership functions of the error signal (e) are optimized (Fig. 8). As shown, the membership functions associated with LN and LP have become very narrow, indicating that the optimization algorithm has significantly reduced their influence.

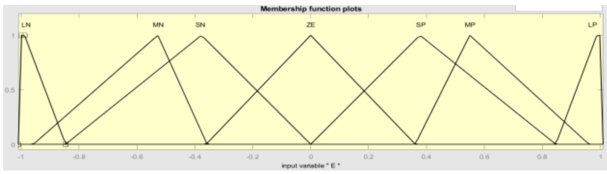

Fig. 8. Optimized membership functions corresponding to the error signal (e)

The membership functions corresponding to the derivative of the error signal ($\dot{e}$) are optimized (Fig.9). As illustrated, the membership functions exhibit a well-ordered structure, indicating that the optimization algorithm has effectively utilized all membership functions.

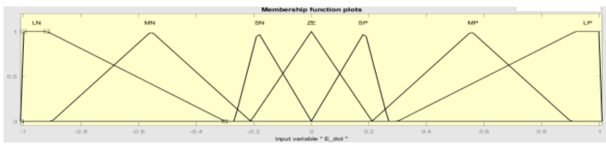

Fig. 9. Optimized membership functions corresponding to the derivative of the error signal ($\dot{e}$)

Also, the output membership functions are optimized (Fig. 10). Similar to the membership functions of $\dot{e}$, the output membership functions exhibit a regular, structured pattern, indicating that the optimizer has effectively used all membership functions.

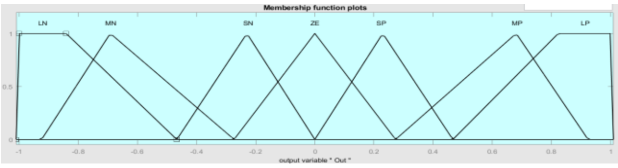

Fig. 10. The optimized membership functions corresponding to the output

After the optimization process, the control surface by the fuzzy rules and membership functions is generated (Fig. 11). It can be observed that the optimization algorithm has introduced noticeable changes to the control surface.

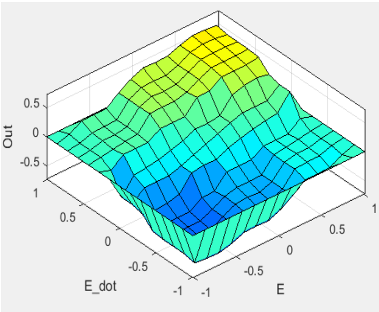

Fig. 11. Optimized fuzzy control output surface

6. Simulation Results

In this section, the simulation results are presented. First, the system is simulated for 100 seconds with a reference power of 7000 W, and the performance of the PID controller and the PSO-optimized fuzzy controller is compared (Fig. 12). As can be observed, the PSO-optimized fuzzy controller achieves better overshoot (8579.34W) rather than the PID controller (8705.03W), faster reaction (11.85s compared to 14.2s), and converges to the reference value in a shorter settling time.

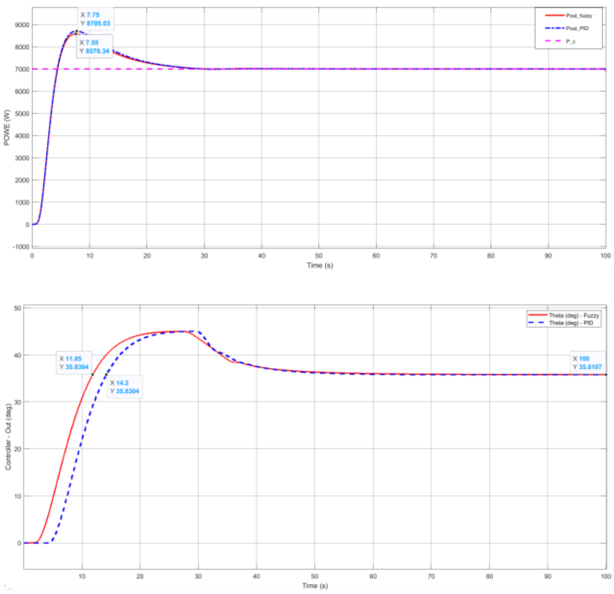

Fig. 12. Power and Controller output with a reference power of 7000w

Next, an additional scenario is designed to provide a more comprehensive comparison between the controllers. As shown in Table III, the simulation scenario is defined as follows. During the time interval from 0 to 100 s, the wind speed is assumed to be constant at 12.5, and the desired power is set to a constant value of 7000. At 100 s, the wind speed remains unchanged, while the desired power decreases from 7000 to 6900 and remains constant over the interval from 100 to 200 s. Subsequently, at 200 s, the wind speed remains constant, whereas the desired power increases from 6900 to 7100 and remains constant from 200 to 300 s. At 300 s, assuming a constant wind speed, the desired power returns to its initial value of 7000 and stays constant over the interval from 300 to 400 s. Finally, after 400 s, the desired power remains at 7000, while the wind behavior changes by adding a sinusoidal component to the constant value of 12.5 to evaluate the controller performance under varying wind conditions.

Table III. The details of the scenario

Time(s)	0-100	100-200	200-300	300-400	400-600
Power_d (w)	7000	6900	7100	7000	7000
Wind speed(m/s)	12.5	12.5	12.5	12.5	12.5+0.1sin(πt/10)

The simulation results corresponding to the defined scenario are shown (Fig. 13). Overall, both controllers successfully handle the scenario. However, as observed at the beginning of the simulation, the optimized fuzzy controller responds faster than the classical controller, achieves a lower overshoot, and maintains the output power at 7000 W with a shorter settling time. When the reference power decreases, both controllers exhibit similar behavior. However, when the reference power increases at 200 seconds, the optimized fuzzy controller effectively tracks the new reference, while the classical PID controller introduces larger oscillations. In this operating point, the optimized fuzzy controller demonstrates superior performance. At 300 seconds, when the reference power decreases again to 7000 W, both controllers successfully regulate the power. Nevertheless, the response of the optimized fuzzy controller is smoother and free of oscillations, indicating better performance.

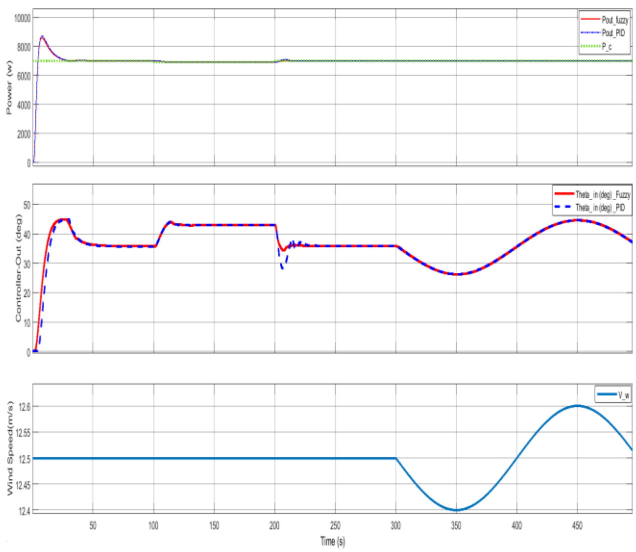

Fig. 13. The results corresponding to the defined scenario

Finally, during the interval from 400 to 600 seconds, while the reference power remains constant and wind speed variations are applied, both controllers maintain satisfactory performance under wind disturbances.

7. Conclusions

This paper presented a systematic comparison between a conventional PID controller and a PSO-optimized fuzzy logic controller for wind turbine power regulation in the pitch region. A detailed nonlinear dynamic model was developed to ensure realistic performance evaluation, incorporating aerodynamic power conversion, pitch dynamics, generator electrical behavior, actuator dynamics, and aerodynamic delays represented by spatial and lag filters. This model provided an accurate framework for assessing controller performance under varying operating conditions.

A dual-loop control architecture was implemented, comprising an inner pitch actuator loop and an outer power control loop. The PID controller served as a benchmark due to its widespread industrial adoption, while the fuzzy logic controller was designed to improve robustness to nonlinearities and wind disturbances. PSO-based tuning of the fuzzy controller parameters enabled systematic optimization with respect to tracking accuracy, transient response, and steady-state performance.

Simulation results under constant and time-varying wind conditions demonstrate that the PSO-optimized fuzzy controller outperforms the PID controller across key metrics, including response speed, overshoot reduction, settling time, and stability. The optimized controller also provides smoother control action and enhanced robustness to wind-speed variations and reference power changes, leading to reduced power oscillations, lower mechanical stress, and improved energy capture efficiency. These findings confirm the effectiveness of optimization-based intelligent control strategies for nonlinear wind energy systems.

Future work will focus on extending the proposed approach to large-scale and offshore wind turbines, incorporating additional drivetrain and structural dynamics, and validating the controller through hardware-in-the-loop simulations and experimental testing.

Acknowledgement

This work has been partially supported by the Spanish Ministry of Science and Innovation under the projects MCI/AEI/FEDER number PID2021-123543OB-C21 and PID2024-155653OB-C21.

References

[1] E. Muñoz-Palomeque, J.E. Sierra-García, and M. Santos, “Intelligent control techniques for maximum power point tracking in wind turbines”, *Revista Iberoamericana de Automática e Informática Industrial*, vol. 21, pp. 193–204, 2024.

[2] A. Eskandari and R. Vatankhah, “Opposition-based particle swarm optimization-aided neural fractional order PID pitch control for variable pitch wind turbines,” *Int J Dyn Control*, vol. 13, no. 6, p. 216, Jun. 2025, doi: 10.1007/s40435-025-01703-9.

[3] W. Wang, Q. Yao, Z. Zhan, K. Sheng, S. Cheng, and Y. Wang, “Variable Pitch Control Based on Fuzzy PI for Semi-Submersible Offshore Floating Wind Turbine,” in *2025 37th Chinese Control and Decision Conference (CCDC)*, IEEE, May 2025, pp. 2041–2046. doi: 10.1109/CCDC65474.2025.11090465.

[4] R. Ma, F. L. Siaw, and T. H. G. Thio, “A Hybrid Fuzzy LQR-PI Blade Pitch Control Scheme for Spar-Type Floating Offshore Wind Turbines,” *J Mar Sci Eng*, vol. 12, no. 8, p. 1306, Aug. 2024, doi: 10.3390/jmse12081306.

[5] B. N. Phung, Y.-K. Wu, and M.-H. Pham, “Novel Fuzzy Logic Controls to Enhance Dynamic Frequency Control and Pitch Angle Regulation in Variable-Speed Wind Turbines,” *Energies (Basel)*, vol. 17, no. 11, p. 2617, May 2024, doi: 10.3390/en17112617.

[6] J. Lin *et al.*, “Fuzzy PID Individual Pitch Control with Effective Wind Speed Estimation for Offshore Floating Wind Turbines,” *Energies (Basel)*, vol. 18, no. 18, p. 4812, Sep. 2025, doi: 10.3390/en18184812.

[7] J. E. Sierra-Garcia and M. Santos, “Combination of fuzzy control and reinforcement learning for wind turbine pitch control,” *Log J IGPL*, vol. 33, no. 5, Aug. 2025, doi: 10.1093/jigpal/jzae054.

[8] J. E. Sierra-Garcia, M. Santos, and R. Pandit, “Wind turbine pitch reinforcement learning control improved by PID regulator and learning observer,” *Eng Appl Artif Intell*, vol. 111, p. 104769, May 2022, doi: 10.1016/j.engappai.2022.104769.

[9] H. Rafia, H. Ouadi, and A. Boulal, “PSO Optimization-Based Control for Floating Offshore wind Turbine: Maximizing Power Generation and Reducing platform motion,” *IFAC-PapersOnLine*, vol. 59, no. 9, pp. 235–240, 2025, doi: 10.1016/j.ifacol.2025.08.142.

[10] H. Ghadiri, M. Sadeghi, A. Abaspour, and R. Esmaelzadeh, “Optimized Fuzzy-Quaternion Attitude control of Satellite in Large maneuver,” in *SpaceOps 2016 Conference*, Reston, Virginia: American Institute of Aeronautics and Astronautics, May 2016. doi: 10.2514/6.2016-2552.

[11] Y. Zhao, X. Yang, Y. Zhang, and Q. Zhang, “Event-Triggered H-Infinity Pitch Control for Floating Offshore Wind Turbines,” *IEEE Trans Sustain Energy*, vol. 16, no. 2, pp. 1329–1339, Apr. 2025, doi: 10.1109/TSTE.2025.3525478.

[12] Y. Zhao, X. Yang, and Z. Zhao, “Pitch control for floating offshore wind turbines via model-dependent extended state observer-based active disturbance rejection control,” *Ocean Engineering*, vol. 316, p. 119883, Jan. 2025, doi: 10.1016/j.oceaneng.2024.119883.

[13] A. Nabeel, A. Lasheen, A. L. Elshafei, and E. Aboul Zahab, “Fuzzy-based collective pitch control for wind turbine via deep reinforcement learning,” *ISA Trans*, vol. 148, pp. 307–325, May 2024, doi: 10.1016/j.isatra.2024.03.023.

[14] C. Liu, Q. Li, C. Wang, T. Xv, W. Gu, and M. Yin, “Active power control of wind turbine based on fuzzy pitch control,” *J Phys Conf Ser*, vol. 2757, no. 1, p. 012018, May 2024, doi: 10.1088/1742-6596/2757/1/012018.